J. Membrane Biol. 113, 75–92 (1990)

The Journal of
Membrane Biology

Increase in Gap Junction Resistance with Acidification in Crayfish Septate Axons Is Closely Related to Changes in Intracellular Calcium But Not Hydrogen Ion Concentration

Camillo Peracchia
Department of Physiology, University of Rochester, Rochester, New York

Summary. Neutral-carrier pH- and Ca-sensitive microelectrodes were used to investigate the relationship between junctional electrical resistance and either pH_i or $[Ca^{2+}]_i$ in crayfish septate axons uncoupled by acidification. For measuring $[Ca^{2+}]_i$ a new neutral carrier sensor sensitive to picomolar $[Ca^{2+}]$ and virtually insensitive to other ions was used. Uncoupling was induced by superfusing the axons with Na-acetate solutions (pH 6.3). With acetate, the time course of changes in junctional resistance differed markedly from that of pH_i or $[H^+]_i$, and $[H^+]_i$ peaked 40–90 sec before junctional resistance. The difference in shape and peak time between pH_i and junctional resistance curves caused significant hysteresis in the pH_i versus junctional resistance relationship. In addition, junctional resistance maxima reached with slow acidification rates were 3–4 times greater than those with fast acidifications of similar magnitude. With acetate, $[Ca^{2+}]_i$ increased by approximately one order of magnitude from basal values of 0.1–0.3 μM. The curves describing the time course of changes in $[Ca^{2+}]_i$ and junctional resistance matched well with each other in shape, peak time and magnitude. Both junctional resistance and $[Ca^{2+}]_i$ recovered following a single exponential decay with a time constant of ~2 min. Different rates of acidification caused increases in $[Ca^{2+}]_i$ and junctional resistance comparable in magnitude. The data indicate that the increase in junctional resistance induced by acidification is more closely related to $[Ca^{2+}]_i$ than to $[H^+]_i$.

Key Words gap junctions · intracellular calcium · intracellular pH · Ca-sensitive microelectrodes · pH-sensitive microelectrodes

Introduction

Gap junction communication between cells is mediated by channels permeable to small cytoplasmic molecules (reviewed in Loewenstein, 1981; Peracchia, 1980, 1987*a*; Ramón & Rivera, 1987). During the past decade, our knowledge of the structure and composition of cell-to-cell channels has improved dramatically, while our understanding of the mechanisms of regulation and modulation of channel permeability has increased only slightly.

The role of Ca^{2+} in the regulation of gap junction channels was first demonstrated by Loewenstein (1966) in perforated salivary gland cells of insects, and later confirmed through experiments that simultaneously monitored changes in electrical coupling and $[Ca^{2+}]_i$, measured with the Ca^{2+}-indicator aequorin (Rose & Loewenstein, 1976). The role of H^+ in gap junction regulation was first proposed by Turin and Warner (1977, 1980) in amphibian embryonic cells in which pH_i, measured with pH-sensitive glass-membrane microelectrodes, and electrical coupling were simultaneously monitored.

Spray, Harris and Bennett (1981) supported the H^+ hypothesis for gap junction regulation by showing that channel conductance of amphibian embryonic cells is a simple and sensitive function of the intracellular pH. This lead them to propose that the changes in conductance are a direct effect of protons on the channels. However, a variety of conflicting data obtained in different cell systems (reviewed in Peracchia, 1987*a*; Ramón & Rivera, 1987) warn against a premature generalization of this theory. While there is solid evidence that Ca^{2+} affects the channels independently from H^+, in most cases it is unclear whether H^+ affects the channels independently from Ca^{2+} (Rose & Rick, 1978).

Supporting a Ca^{2+}-mediated effect of H^+ on the channels is evidence for a calmodulin (CaM) involvement in channel regulation. The CaM hypothesis for coupling regulation (reviewed in Peracchia, 1988) is based on the capacity of CaM inhibitors to prevent low pH_i-induced cell uncoupling in amphibian embryos (Peracchia, Bernardini & Peracchia, 1983; Peracchia, 1984) and in crayfish septate axons (Peracchia, 1987*b*), and on the capacity of Ca^{2+}-activated CaM to close gap junction channels incorporated into liposomes (Girsch & Peracchia, 1985) and to uncouple internally perfused crayfish axons (Arellano et al., 1988).

In order to study the relationship between junctional conductance and both pH_i and $[Ca^{2+}]_i$ we have simultaneously measured either pH_i or pCa_i and both junctional and surface membrane resistances in crayfish septate axons. These axons provide a two-cell system where the junctional resistance (R_j) can be carefully quantitated for periods as long as 8 to 10 hr with a four microelectrode system (Peracchia, 1987*b*). Data from this study indicate that in crayfish axons gap junction resistance is closely related to changes in $[Ca^{2+}]_i$ but not to changes in $[H^+]_i$. A preliminary account of this study has been published (Peracchia, 1989*a*).

Materials and Methods

Experimental Preparation

Crayfish (*Procambarus clarkii*) of either sex, approximately 10 cm long were obtained from Carolina Biological Supply, Burlington, NC, and kept in a well oxygenated aquarium equipped with a recirculating-filtering water system at 22–24°C. The animals were anesthetized by cooling and sacrificed by decapitation. The ventral nerve cord was removed and pinned, dorsal side up, to a petri dish lined with Sylgard (Dow Corning, Midland, MI) and filled with saline (*see below*). The sheath of connective tissue enveloping the nerve cord was carefully removed with scissors from the dorsal side of the cord and a segment of the cord comprising three ganglia was cut off and pinned dorsal side up to a Plexiglas chamber lined with Sylgard. Either the third or fourth abdominal ganglion was used.

The chamber was continuously perfused by a peristaltic pump (Micro Perpex, Pharmacia LKB Biotechnology, Pisicataway, NY), at a flow rate of 1 ml/min (unless stated otherwise), with a standard saline solution for crayfish (SES) (Johnson & Ramón, 1981) containing (in mM): NaCl, 205; KCl, 5.4; $CaCl_2$, 13.5 and HEPES, 5 (pH 7.5). The level of the solution in the chamber was maintained constant by continuous suction through a glass pipette, such that at any time during the experiment the chamber contained ~1.3 ml of fluid. Electrical uncoupling was obtained by superfusing the axons for 3 or 5 min, at the same flow rate, with a sodium acetate saline solution (Ac) containing (in mM): Na acetate, 205; KCl 5.4 and $CaCl_2$, 13.5 (pH 6.3). In some experiments the axons were superfused with sodium-free solutions (zero-Na^+) obtained by substituting all the NaCl in SES with tetramethylammonium chloride (TMA). All experiments were performed at 22–24°C.

Electrical Measurements

For passing current and measuring voltages, microelectrodes were pulled from borosilicate glass capillaries 1.2 mm (OD) 0.68 mm (ID) (Kwik fill, W-P Instruments, New Haven, CT) by means of a Brown-Flaming Micropipette puller (Sutter Instruments, San Francisco, CA). The microelectrodes, filled with a 2.5 M KCl solution (pH 7) had a resistance of 8–10 MΩ in SES. Four microelectrodes were inserted into a lateral giant axon, two on each side of the septum (Fig. 1*A*). The bath was grounded with a silver-silver chloride reference electrode connected to the superfusion chamber via an agar-SES bridge.

Constant current pulses were generated by an IBM XT computer coupled to a D/A converter (Model DT 2801, Data Translation, Marlborough, MA) and to a voltage to current converter (701M amplifier, WPI) (Fig. 1*A*). Hyperpolarizing current pulses (150 nA, 300 msec duration) were injected through current microelectrodes (I_1, I_2) every 10 sec alternatively into the posterior (C_1) and anterior (C_2) axonal segment (Fig. 1). The resulting electronic potentials V_1 and V_2 (from current injection in C_1), and V_{1*} and V_{2*} (from current injection in C_2) as well as the membrane potentials (E_1 and E_2) were recorded with two voltage microelectrodes connected to a voltage follower (AM-4 amplifier, Biodine, Electronics, Santa Monica, CA). The voltage signals were displayed on a storage oscilloscope (5113, Tektronix, Beaverton, OR) and on a chart recorder (2200, Gould, Cleveland, OH), and were digitized and stored both on the hard disc of the IBM computer and on the tape of a stereo VHS-VCR coupled to a PCM2 (Medical Systems Corp., Greenvale, NY) (Fig. 1*A*).

Ion-Selective Microelectrodes

Batches of 20–30 microelectrodes identical to those used for passing current and recording voltage (*see above*) were baked in an oven at 200°C for 1 hr, under a metal can. The microelectrodes were silanized at 200°C by exposure to vapors of dimethyltrimethylsilylamine (Fluka Chemical, Ronkonkoma, NY), injected (50–200 μl) through a small hole in the metal can. Ten minutes later the can was removed, and the microelectrodes were baked for a further 30 min. The microelectrodes were stored in a desiccator for periods not greater than one week.

pH-sensitive microelectrodes were backfilled with a filtered 2.5 M KCl solution buffered to pH 7 with 20 mM HEPES. The electrolyte solution was forced to fill the shank and the tip of the silanized microelectrodes by applying back pressure with a syringe. The movement of the solution was monitored through a compound microscope and, immediately after the solution had reached the tip, the microelectrodes were dipped into a proton-cocktail (Fluka) based on the neutral carrier tri-*n*-dodecylamine (Ammann et al., 1981). A short column of cocktail (<100 μm) was allowed to enter the tip; in some instances, moderate suction was necessary. Before use, the shank and the tip of the microelectrodes were examined under the microscope at 400 × magnification to determine the absence of contaminants and air bubbles.

pH microelectrodes were calibrated by passing through the chamber (at 1 ml/min) 220 mM KCl solutions buffered to pH 6, 7 and 8 with 20 mM phosphate. The voltage signal (V_m) from a reference microelectrode (filled with 2.5 M KCl) was passed through the voltage follower (AM-4, Biodine) and that (V_{ion}) from the pH electrode was passed through a high impedance amplifier (FD 223 Electrometer, WPI). Both V_m and ($V_{ion} - V_m$) (Fig. 2*A*) were displayed on the chart recorder. The electrode response ranged from 50 to 55 mV per pH unit. For testing the response time, the tips of pH microelectrodes were placed at the opening of a small polyethylene capillary obliquely cut. pH buffers were pumped through the capillary at a rate of 2.7 ml/min. Most pH microelectrodes had a 50% response time ranging from 7 to 8 sec (Fig. 2*B*). The same response time was observed with acetate solutions of different pH.

For testing possible effects of changes in $[Ca^{2+}]$ and of replacement of Cl^- by acetate on pH microelectrodes, solutions of pH 7 buffered to either pCa 7 (5 mM EGTA, 1.63 mM $CaCl_2$; 205 mM Na-acetate) or pCa 5 (5 mM EGTA, 4.9 mM $CaCl_2$, 205 mM Na-acetate), and solutions buffered to pH 6.3 (5 mM EGTA, 10 mM MES) containing either NaCl or Na-acetate (205 mM) were

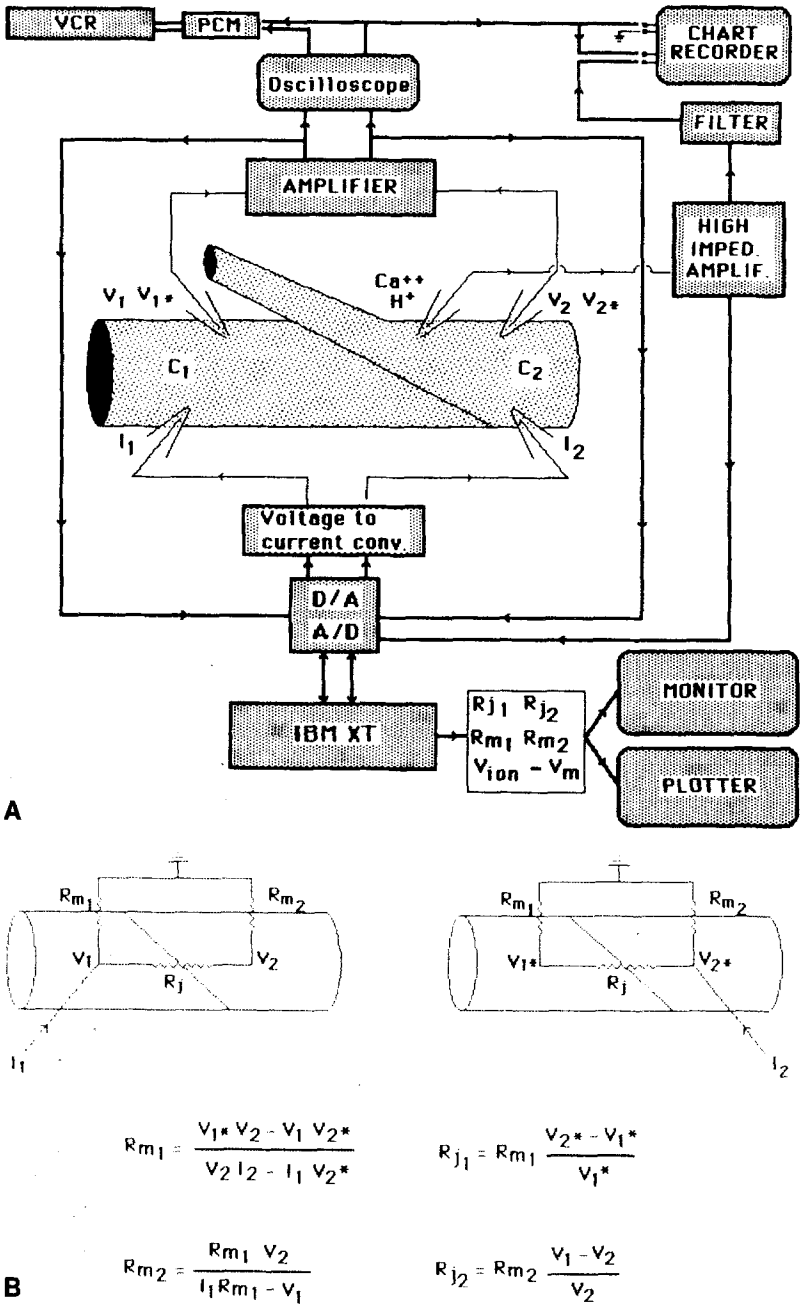

Fig. 1. Diagram of electrical recording set-up. (*A*) Hyperpolarizing current pulses generated by the computer coupled to *D/A* and voltage-to-current converters, are injected through current microelectrodes (I_1, I_2) alternatively in the posterior (C_1) and anterior (C_2) axon segments. The resulting potentials (V_1, V_2, V_{1*}, V_{2*}), sampled with two voltage microelectrodes, are passed through the amplifier, stored on the computer's hard disc and the VCR tape, and displayed in the chart recorder and the oscilloscope. The voltage signal (V_{ion}), recorded by the ion selective microelectrode (H^+ or Ca^{2+}) either in the posterior or anterior axon as closely as possible to the septum, is passed through the high impedance amplifier, filtered and continuously displayed in the chart recorder after subtraction of membrane potential (V_m). At 10-sec intervals V_{ion} is also sampled by the computer (100 msec before each current pulse), stored unfiltered on the hard disc and plotted on-line on the monitor as $V_{ion}-V_m$. (*B*) Equivalent circuit and equations (Bennett, 1966) used to calculate junctional (R_{j1}, R_{j2}) and nonjunctional (R_{m1}, R_{m2}) resistances. Both R_{j1} and R_{j2} were continuously plotted on line on the monitor (*A*)

passed through the calibration chamber. Neither the change in $[Ca^{2+}]$ nor the replacement of acetate for Cl^- had a significant effect on the pH^- electrode response. This confirms previous data reporting an extremely high selectivity of this proton-cocktail with respect to Ca^{2+}, Na^+, and K^+, when evaluated with the fixed interference method (Schulthess et al., 1981).

Ca^{2+}-sensitive microelectrodes were prepared similarly to pH-microelectrodes using a recently developed calcium-cocktail (ETH 129, Schefer et al., 1986) (Fluka Chemical, Ronkonkoma, NY). The cocktail contains the Ca^{2+} ionophore N,N,N',N'-tetracyclohexyl-3-oxapentanediamide, which forms an ideal coordination sphere of nine oxygen atoms for Ca^{2+} uptake (Schefer et al., 1986). Ca-microelectrodes prepared with this cocktail have a logarithmic response down to $[Ca^{2+}]$ of 5×10^{-10} M and are virtually insensitive to other cytoplasmic ions (Ammann et al., 1987). The microelectrodes were backfilled with Ca solutions buffered with EGTA (*p*Ca7; Alvarez-Leefmans, Rink & Tsien, 1981) or citrate (pH7) and containing 220 mM KCl.

The Ca^{2+} sensitivity and response time of the microelectrodes were tested as described above. For calibration, two types of Ca-buffered solutions (*p*Ca 5, 6, 7 and 8) were used. One contained (in mM): EGTA, 10; $CaCl_2$, 5; KCl, 220; and either MES, 10 (pH, 6.15; *p*Ca, 5) or PIPES, 10 (pH, 6.65; *p*Ca, 6) or MOPS, 10 (pH, 7.15; *p*Ca, 7) or HEPES, 10 (pH, 7.66; *p*Ca, 8). The other (Alvarez-Leefmans et al., 1981) contained (in mM): $CaCl_2$, 5; KCl, 220; and either NTA, 10 and TAPS, 10 (pH, 8.42;

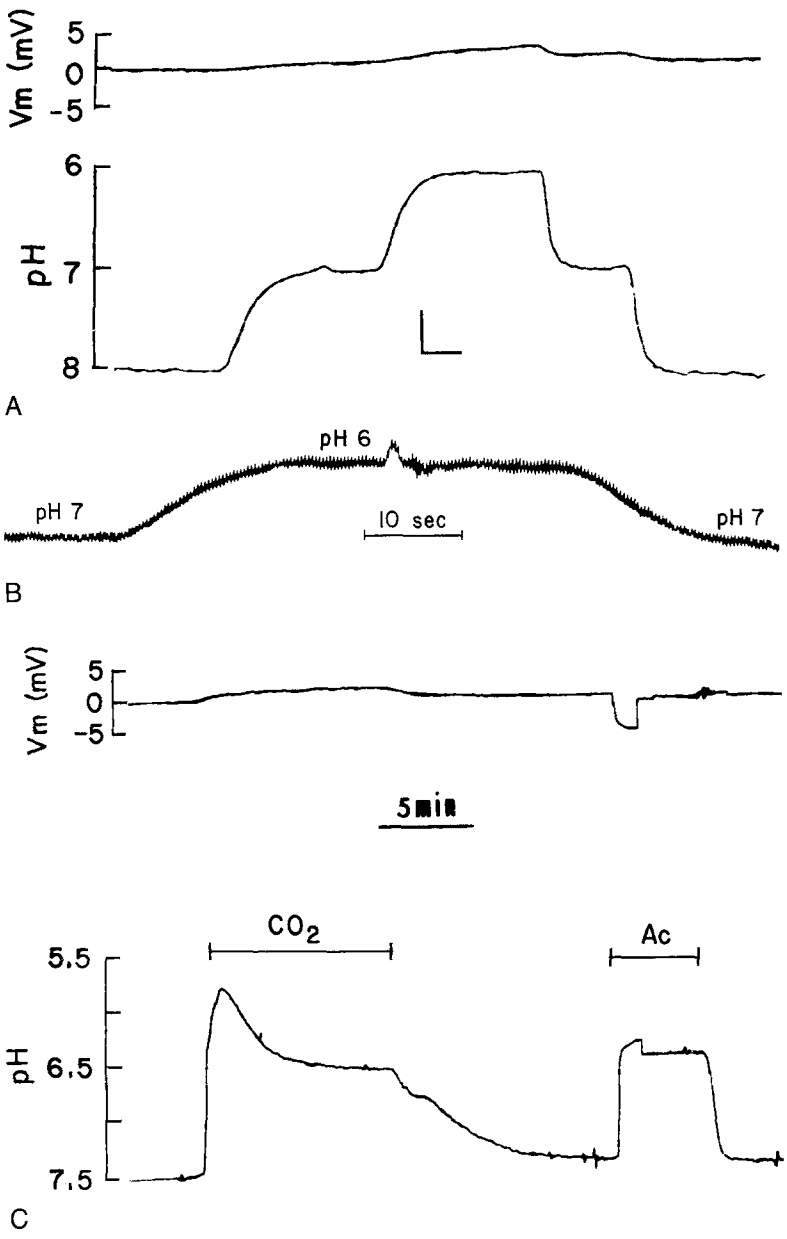

Fig. 2. (*A*) Calibration of a neutral carrier pH-sensitive microelectrode in 220 mM KCl solutions buffered to pH 6, 7 and 8 with 20 mM phosphate. The upper trace shows the voltage of the reference electrode (V_m). The lower trace, the voltage of the pH microelectrode after subtraction of V_m. (Vertical bar = 20 mV; horizontal bar = 1 min). (*B*) Calibration of pH-microelectrode response time. The microelectrode was placed at the opening of a small capillary perfused with buffered KCl solutions (pH 6 and 7) at a flow of 2.7 ml/min. Electrodes typically had a 50% response time of ~7.5 sec. The rhythmic spikes superimposed on the tracing are an artifact caused by the peristaltic pump. (*C*) Test of pH microelectrode sensitivity to CO_2 and Ac in the superfusion chamber. The chamber was successively perfused with SES, SES-CO_2, SES, Ac and SES at a flow of 1 ml/min. Upon perfusion with SES bubbled with 100% CO_2 (CO_2) pH decreases rapidly at first (but less than expected) and then partially recovers while still in CO_2. Upon return to SES, pH recovery appears to be slow and incomplete, taking 10–12 min, while in fact a complete CO_2 washout occurs in ~90 sec. Upon perfusion with acetate (Ac), the microelectrode monitors a rapid acidification to pH 6.3. This pH value is maintained constant during Ac perfusion and then recovers quickly to pH 7.5 with SES perfusion. The unusual behavior of pH microelectrodes with CO_2 is due to diffusion of CO_2 through the proton cocktail. The upward step in the pH tracing during Ac perfusion is an artifact caused by voltage shift in the reference electrode (*see* upper trace)

*p*Ca, 5) or HEEDTA, 10 and HEPES, 10 (pH, 7.70; *p*Ca, 6) or EGTA, 10 and MOPS, 10 (pH, 7.29; *p*Ca, 7) or EGTA, 10 and HEPES, 10 (pH, 7.80; *p*Ca, 8). The Ca-buffered solutions were flowed through the chamber at a rate of 1 ml/min and both V_m and V_{ion}–V_m were recorded as described above. The electrode response ranged 15–25 mV per *p*Ca unit (Fig. 3*A*). The response time of the Ca-microelectrodes was measured as described for the pH-microelectrodes. Ca-microelectrodes typically had a 50% response time of ~14 sec (Fig. 3*B*).

For testing possible effects of changes in pH and of replacement of Cl^- by acetate on Ca-microelectrodes, 1 mM Ca^{2+} solutions buffered either to pH 7.5 (20 mM HEPES) or to pH 6 (20 mM MES), and 13.5 mM Ca^{2+} solutions containing either NaCl or Na-acetate (205 mM) were passed through the calibration chamber. Figure 3*C* shows that a pH change from 7.5 to 6 causes a 2-mV positive voltage step, corresponding to a H^+ sensitivity of ~1.3 mV per pH unit. Thus, the sensitivity of Ca^{2+} microelectrodes to H^+ is only ~3% of that to Ca^{2+}. The sensitivity of this Ca^{2+}-neutral carrier to H^+ has been reported to be more than two orders of magnitude lower than that to Ca^{2+} (Ammann et al., 1987). Replacement of NaCl with Na-acetate had no effect on the Ca^{2+}-electrode response (*data not shown*).

The sensitivity of the ion-selective microelectrodes was tested both before and after the experiments. In a few cases the electrodes could not be tested at the end of the experiment because of the loss of the neutral carrier cocktail either before or during withdrawal from the cell. In these cases, only records showing stable baseline and consistent response to acidification throughout the length of the experiment were saved and analyzed. The ion-selective microelectrodes were inserted into either one of the two axon segments, as closely as possible to the septum. For testing possible differences between the two cells,

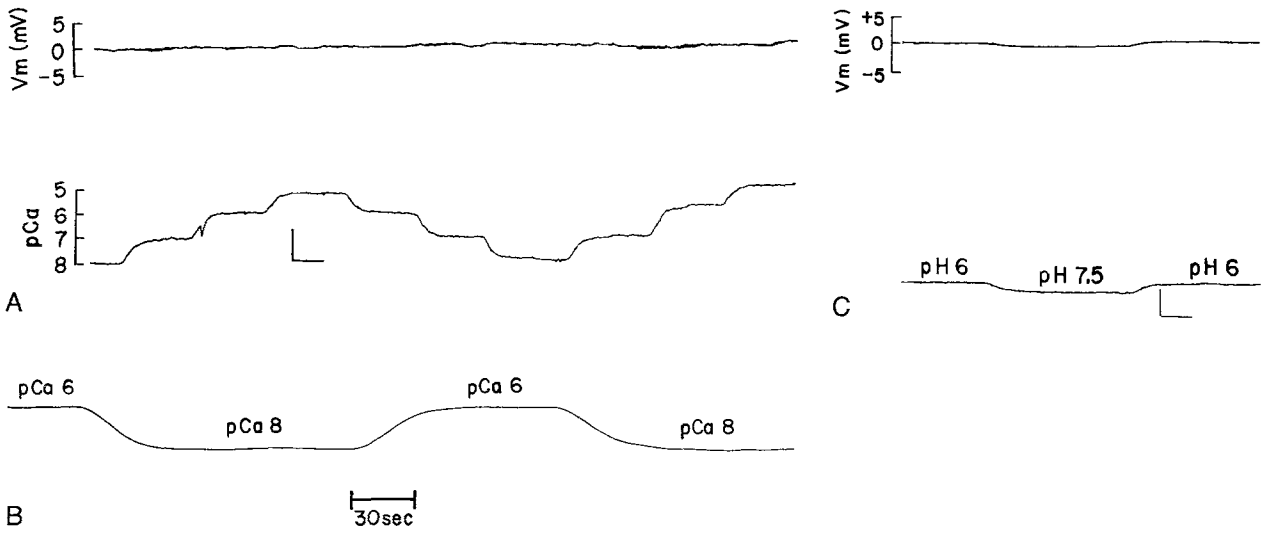

Fig. 3. (*A*) Calibration of neutral carrier Ca-sensitive microelectrode in 220 mM KCl solutions buffered to *p*Ca 5, 6, 7 and 8. The upper trace shows the voltage of the reference electrode (V_m). The lower trace, the voltage of the Ca-microelectrode after subtraction of V_m (vertical bar= 20 mV; horizontal bar = 2 min). (*B*) Calibration of Ca-microelectrode response time. Electrodes typically had a 50% response time of ~14 sec. (*C*) Test of Ca-microelectrode sensitivity to H^+. The chamber was successively perfused with 1 mM [Ca^{2+}] solutions buffered either to pH 6 or to pH 7.5. The microelectrode response was 1.3 mV per pH unit. This microelectrode had a Ca^{2+} sensitivity of 22 mV per *p*Ca unit. (Vertical bar = 5 mV; horizontal bar = 1 min)

in some experiments the ion-selective microelectrodes were moved back and forth from one to the other axon segment.

Analysis of Data

Both membrane (R_{m1}, R_{m2}) and junctional (R_{j1}, R_{j2}) resistances were calculated and plotted on-line on the computer monitor by means of a program written in ASYST language (Adaptable Laboratory Software, Rochester, NY). The resistances were calculated from current and voltage records using the π-t transform (Bennett, 1966) (Fig. 1*B*).

The voltage signal detected by the ion-selective microelectrodes was passed through the high impedance amplifier, filtered (0.1 Hz) and displayed on the pen recorder after subtraction of membrane potential ($V_{ion} - V_m$) (Fig. 1*A*). At 10-sec intervals, the voltage signal of the ion selective microelectrodes was also sampled by the computer, 100 msec before each current pulse. The voltage signal was digitized, stored unfiltered on the hard disc and plotted on-line as ($V_{ion} - V_m$) (Fig. 1*A*).

Artifactual Behavior of pH Electrodes in CO_2 Solutions

Both in the bath (Fig. 2*C*) and in the axons (*data not shown*) the pH electrodes displayed an unusual behavior when exposed to superfusing solutions bubbled with 100% CO_2. A rapid decrease in pH, smaller than expected, was followed by partial pH recovery long before the end of the CO_2-superfusion (Fig. 2*C*). At the end of the CO_2 exposure, a return toward pH 7.5 (SES) appeared to occur gradually and incompletely in the bath over 10–12 min (Fig. 2*C*), while in fact a complete CO_2 washout takes place in ~90 sec. In the axon, at the end of the CO_2 superfusion pH increased at first above pH 7.5 and then slowly decreased to pH ~7.2 (slightly more acid than before the CO_2 exposure). In contrast, acidification caused by superfusion with the AC solution (pH 6.3) resulted in the expected changes in pH in terms of both magnitude and time course (Fig. 2*C*).

A reasonable explanation of the artifactual behavior of the pH electrodes in 100% CO_2 is that CO_2 slowly diffuses in and out of the microelectrode, through the neutral carrier cocktail, and consequently changes the pH of the microelectrode filling solution. In our microelectrodes the filling solution was buffered to pH 7 with 20 mM HEPES. While a stronger pH buffering of the filling solution might have reduced the artifactual effect of CO_2, we chose to avoid entirely the use of CO_2. Acetate substitution of chloride proved to be the treatment of choice, not only because acetate does not alter the behavior of the pH electrode but also because the acetate-induced pH_i changes are very consistent in both magnitude and time course (*see below*).

Results

Crayfish septate axons are an excellent two-cell system for studying electrical uncoupling for several reasons. First of all, the axons survive in vitro for many hours, maintaining membrane potentials ranging from −80 to −90 mV; secondly, the junctional response to acidification is remarkably consistent within a given preparation in terms of magnitude of R_j changes, time course and reversibility (Fig. 4*C*). In different preparations, however, the same acidifying treatment can cause changes in R_j of different magnitude. While in most cases a 3–5 min superfusion of AC at a flow rate of 1 ml/min causes a 50–200% increase in R_j (*see* Fig. 7), in

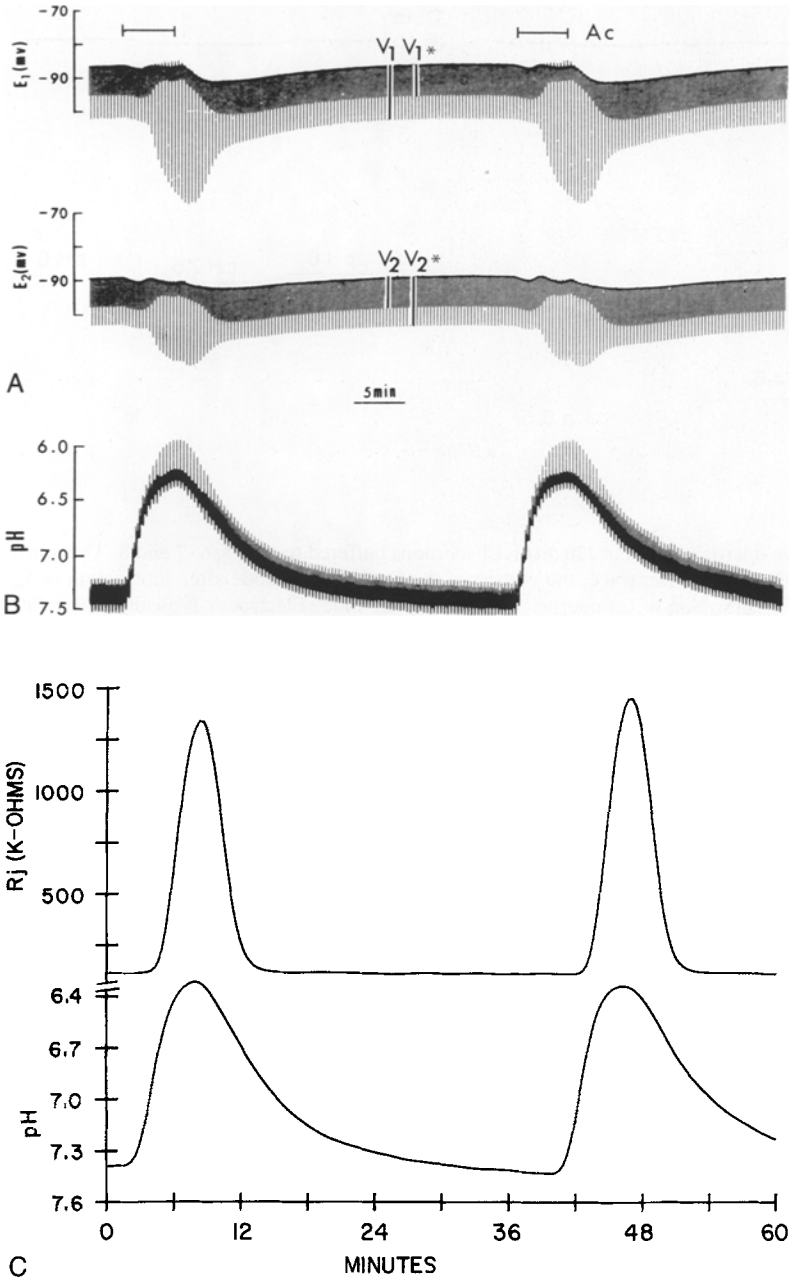

Fig. 4. Time course of changes in electrotonic potentials, R_j and pH_i in crayfish septate axons uncoupled with Ac. (*A*) Low speed chart recording of membrane and electrotonic potentials in the posterior (upper tracing) and anterior (lower tracing) axon segment. Hyperpolarizing square current pulses (150 nA, 300 msec) are injected every 10 sec alternatively into the anterior and posterior axon segment. With Ac superfusion V_1 and V_{2*} increase and V_{1*} and V_2 decrease in amplitude, due to an increase in R_j. (*B*) Low speed chart recording of pH_i continuously monitored in the anterior axon and plotted as $V_{ion}-V_m$ after filtering (0.1 Hz). (*C*) Computer calculated changes in R_j and pH_i; pH_i was sampled unfiltered by the computer every 10 sec (100 msec before current pulses) and plotted after subtraction of membrane potential. Note differences in time course and peak time between R_j and pH_i changes

some axons the same treatment can cause a 500–900% increase in R_j (Fig. 4*C*). These axons usually have control R_m values greater than 100 kΩ and most often are found in animals sacrificed during the winter months. The large differences in R_j maxima among axons does not reflect differences in pH_i minima. In fact, in all the experiments pH_i consistently decreased from control values of ~7.3 to minima ranging from 6.15 to 6.25 (Figs. 4*B* and *C*; *see also* Figs. 7*B* and *C*, and 8*A*).

Changes in R_j and pH_i with Acidification

Upon superfusion with acetate-containing saline solutions (Ac) the amplitudes of V_1 and V_{2*} increase, while those of V_2 and V_{1*} decrease (Fig. 4*A*), reflecting an increase in R_j (Fig. 4*C*). The R_j curve is almost symmetrical (Fig. 4*C*), the recovery phase being only very slightly slower towards the end, and the time course of the R_j changes is remarkably consistent. This is demonstrated by a computer-

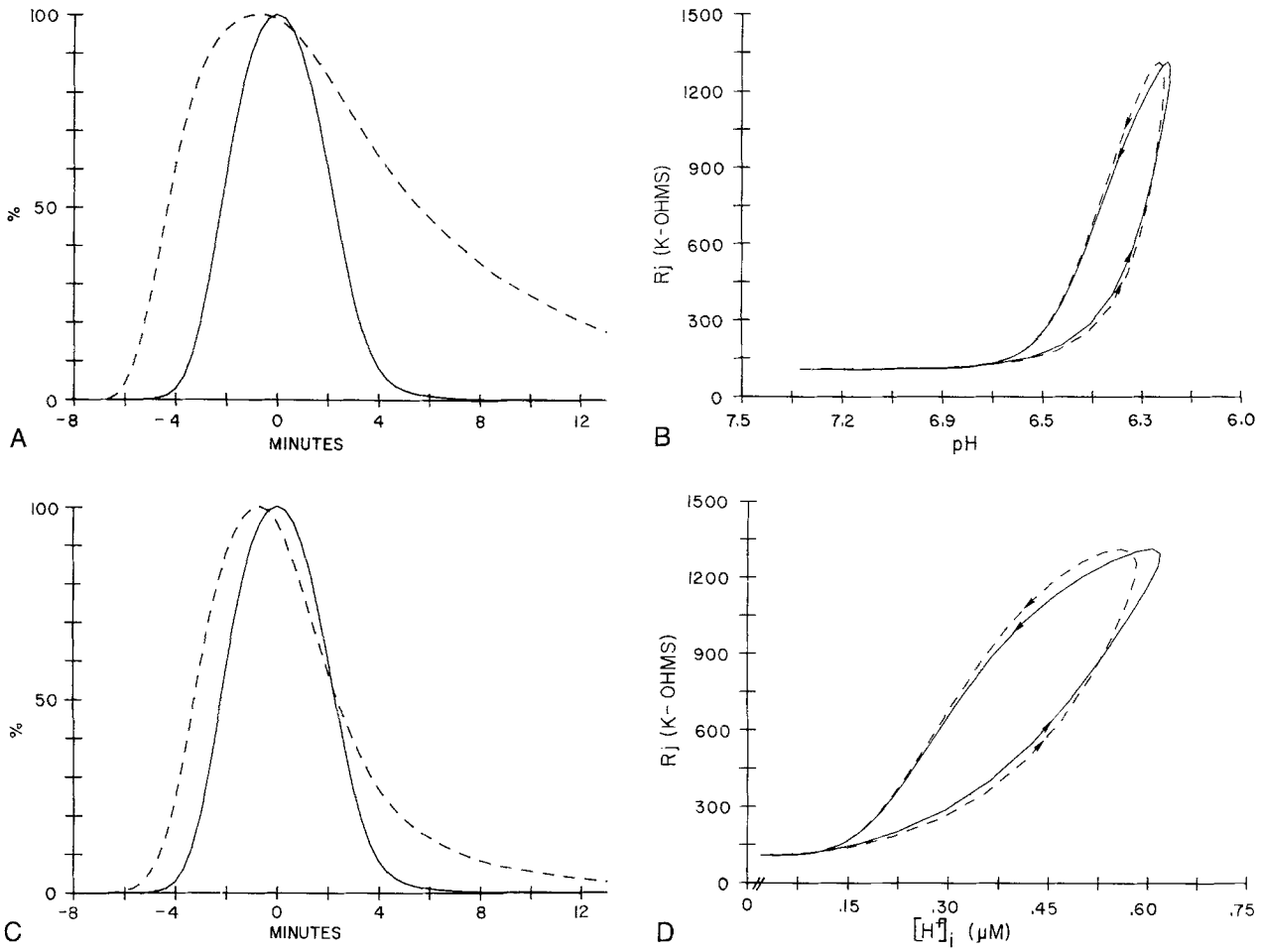

Fig. 5. (*A*) Time course of percent changes in pH_i (dashed line) and R_j (solid line) with Ac (from experiment shown in Fig. 4, II Ac). Note that R_j and pH_i peaks are separated by ~1 min, and the two curves differ substantially in shape. (*B*) Relationship between pH_i and R_j during the I (solid line) and II (dashed line) Ac of Fig. 4. The difference in peak time and curve shape between pH_i and R_j (*A*) causes significant hysteresis in the pH_i–R_j relationships. The arrowheads indicate the temporal sequence of uncoupling (arrowhead pointing up) and recoupling (arrowhead pointing down). (*C*) Time course of percent changes in $[H^+]_i$ (dashed line) and R_j (solid line) with Ac (II Ac of Fig. 4). Note that $[H^+]_i$ and R_j curves differ substantially in shape and peak time. (*D*) The relationship between $[H]_i$ and R_j during the I (solid line) and II (dashed line) Ac of Fig. 4 shows marked hysteresis in the recoupling versus uncoupling phase

generated superposition of several R_j curves from experiments using either 3 min (Fig. 6*A*) or 5 min (Fig. 6*C*) Ac superfusions.

In contrast with the symmetrical shape of R_j curves, both pH_i (Fig. 4*C*) and $[H^+]_i$ (Fig. 5*C*) curves are always asymmetrical. pH_i decreases rapidly with Ac (1 ml/min) at a maximum rate of 0.41 pH units/min but it recovers at a much slower rate. Both the magnitude and time course of the pH_i changes are quite consistent in different experiments (Fig. 6*B* and *D*). The large difference in recovery rate between pH_i and R_j is not due to the logarithmic function of pH, as it is very marked also when $[H^+]_i$ rather than pH_i curves are compared with R_j curves (Fig. 5*C*). In this case, $[H^+]_i$ decreases following a single exponential decay with a time constant (τ) of ~4.4 min, while R_j recovers with a τ = ~2 min.

R_j and pH_i (or $[H^+]_i$) curves also differ substantially in peak time. Plots of the time course of both R_j and pH_i or $[H^+]_i$ show that the peaks of pH minima (Fig. 5*A*) or $[H^+]_i$ maxima (Fig. 5*C*) precede the peaks of R_j maxima by 40–90 sec. The differences in both curve shape and peak time between pH_i and R_j curves result in marked curve hysteresis in the relationship between R_j and either pH_i (Fig. 5*B*) or $[H^+]_i$ (Fig. 5*D*), such that, at the same pH_i, R_j is much greater during recoupling than during uncoupling (Fig. 5*B*). In addition, due to difference in peak time between pH_i and R_j, one sees R_j still rising when $[H^+]_i$ is already decreasing (Figs. 5*B* and *D*, and 7*D*).

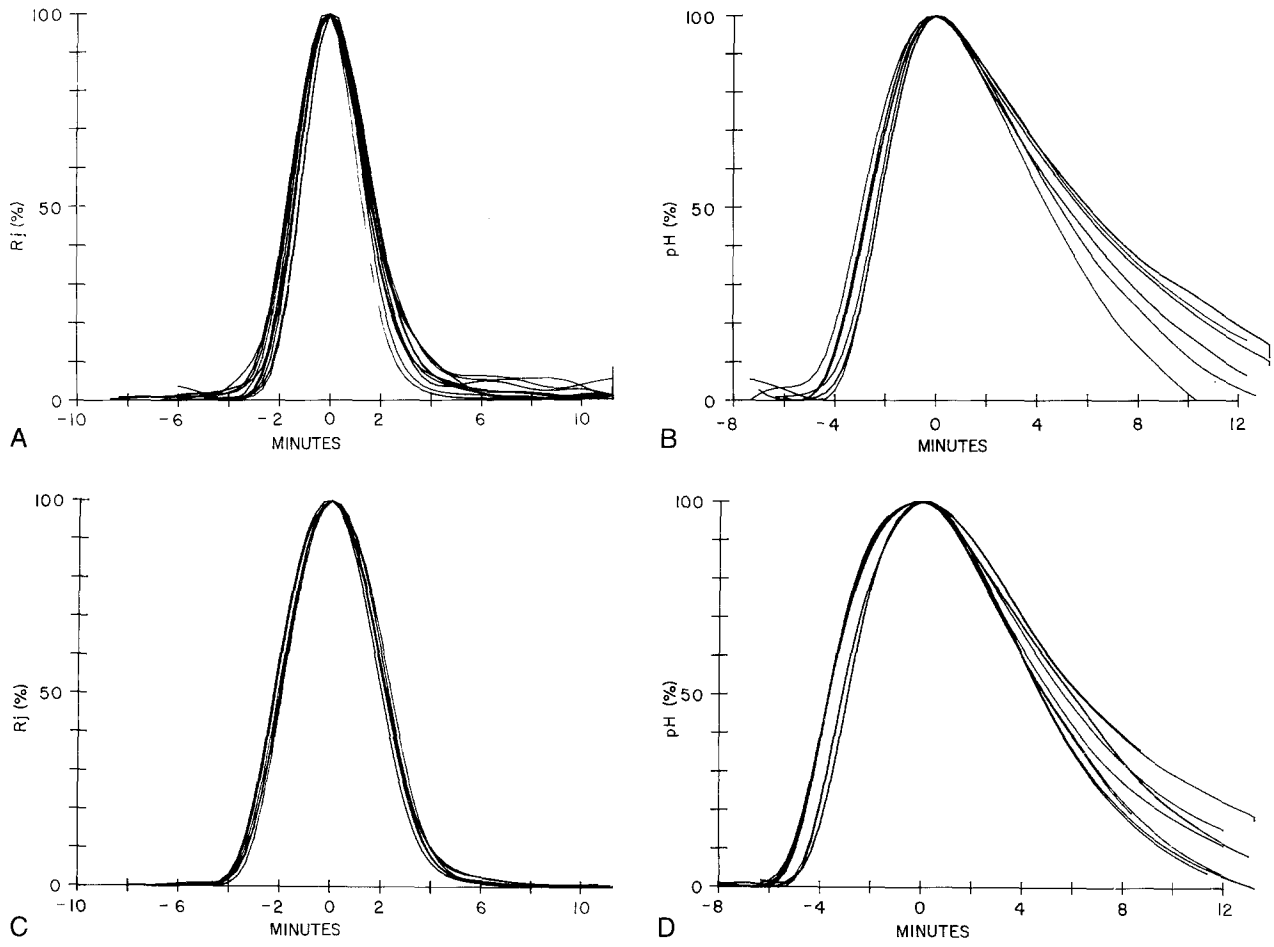

Fig. 6. Computer generated superimposition of several curves, from different experiments, describing the time course of percent changes in R_j and pH_i with Ac treatments of 3 (*A* and *B*) or 5 (*C* and *D*) min duration. All the curves were normalized by plotting the maxima at time zero. Note the consistency of pH_i and R_j behavior in different experiments. R_j and pH_i curves differ substantially in shape: R_j curves are almost symmetrical while pH_i curves show fast rise and slow decay. The slight divergence among the R_j curves (*A*) is due, in part, to small variations in the level of the solution in the perfusion chamber among experiments. This causes slight differences in both the onset and recovery rates of the Ac effects

R_j AND pH_i FOLLOWING DIFFERENT RATES OF ACIDIFICATION

To study the effects on R_j of cytoplasmic acidifications different in rate but similar in magnitude, various experimental protocols involving different superfusion flow rates and different durations of Ac exposure were tested. It was found that the same pH_i minima obtained by superfusing Ac for 3 min at a flow rate of 1 ml/min (II and IV Ac treatment in Fig. 7*B* and *C*) could be obtained by superfusing Ac for 130 sec at a rate of 2 ml/min (I and III Ac treatment in Fig. 7*B* and *C*). By doubling the normal flow rate, the maximum rate of cytoplasmic acidification increases to 0.52 pH units/min (27% greater than in controls; note the steeper pH_i slope in Fig. 7*B* and *C*), the same pH minimum (pH_i = ~6.15) is obtained, although it lasts a shorter time (note the sharper peak of pH in Fig. 7*B* and *C*), and the rate of recovery increases by approximately 20%. In contrast with the consistency of pH_i minima achieved with this protocol, the R_j maxima obtained with slow acidifications are three times greater than those resulting from fast acidifications of the same magnitude (Fig. 7*C*). A marked hysteresis in the pH_i–R_j relationship is also apparent, as previously described, in both fast and slow acidification experiments (Fig. 7*D*).

R_j AND pH_i IN ZERO-Na_o^+ SOLUTIONS

To test for the possible requirement for external Na^+ in the recovery of normal pH_i following Ac-induced acidification, some axons were superfused

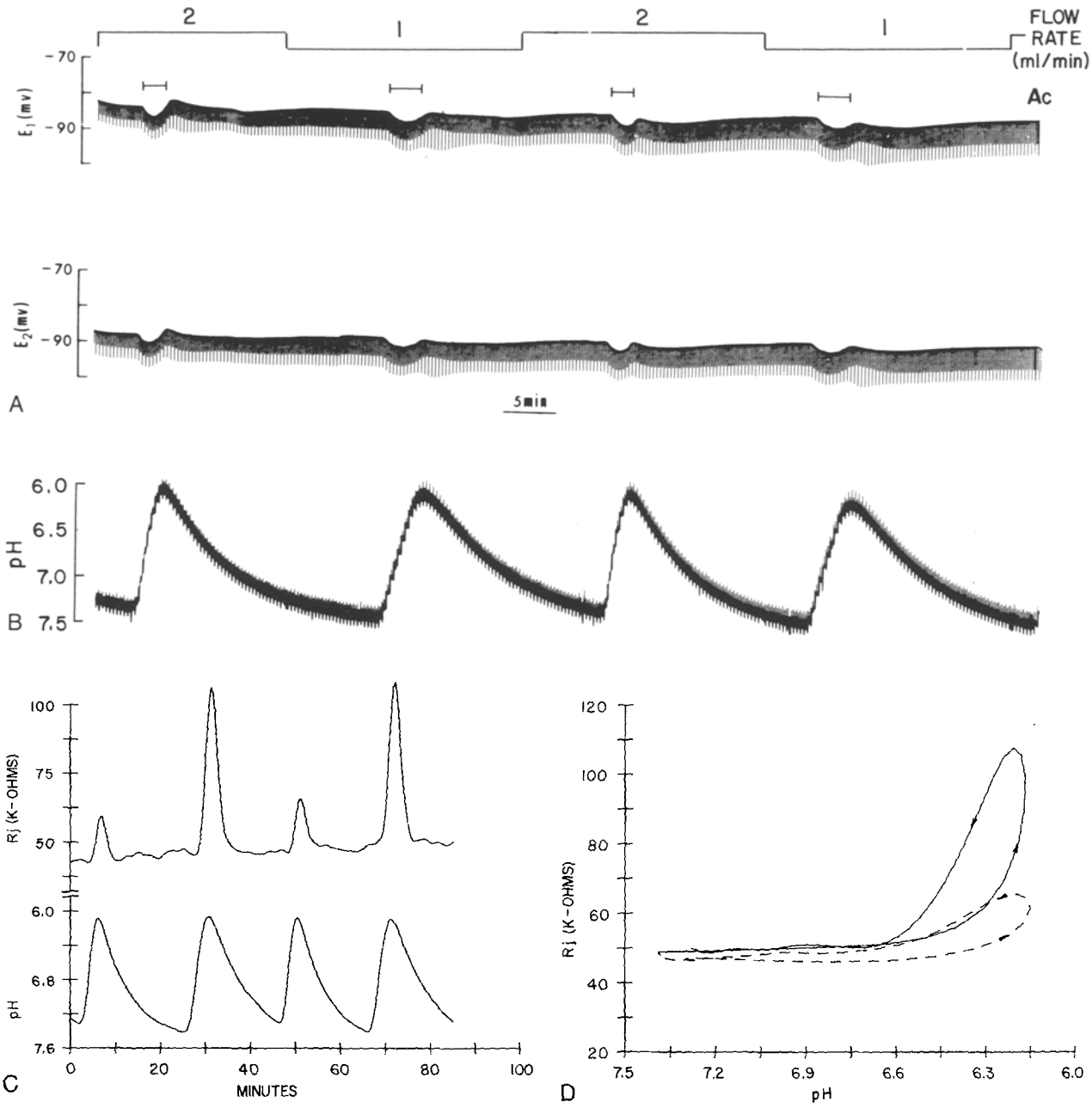

Fig. 7. (*A* and *B*) Low speed chart recording of electrotonic potentials (*A*) and pH_i (*B*) in crayfish septate axons subjected to different rates of acidification. The axons were superfused at a flow rate of either 1 or 2 ml/min. Similar pH_i minima (*B*) were obtained with either 3 min Ac superfusions at 1 ml/min (II and IV Ac) or 130 sec Ac superfusions at 2 ml/min (I and III Ac). (*C*) Time course of changes in R_j and pH_i in the four Ac-induced uncoupling events shown in *A* and *B*. Note that the R_j maxima obtained with slow pH_i changes (II and IV) are 350% greater than those obtained with fast pH_i changes of similar magnitude (I and III). (*D*) pH_i–R_j relationship in the III (dashed line) and IV (solid line) uncoupling event. Note a significant hysteresis in the pH_i–R_j curves for both fast and slow acidification

with zero-Na^+ recovery solutions (Na^+ substituted with TMA), rather than SES, following Ac treatments (Fig. 8*A*). With zero-Na^+ recovery solutions, pH_i decreases only slightly more (pH = 6) than in the control (pH = 6.15) and the minimum pH value lasts a few seconds longer than in controls (Fig. 8*A* and *B*), but the recovery rate is not significantly altered (Fig. 8*B*). In fact, in both cases $[H^+]_i$ decreases following a single exponential decay with a τ ranging from 4.3 to 4.6 min. This indicates that recovery from Ac acidification is not significantly dependent on Na^+/H^+ exchange. This finding, together with the observed consistency in time course and in magnitude of pH_i changes, indicates that the

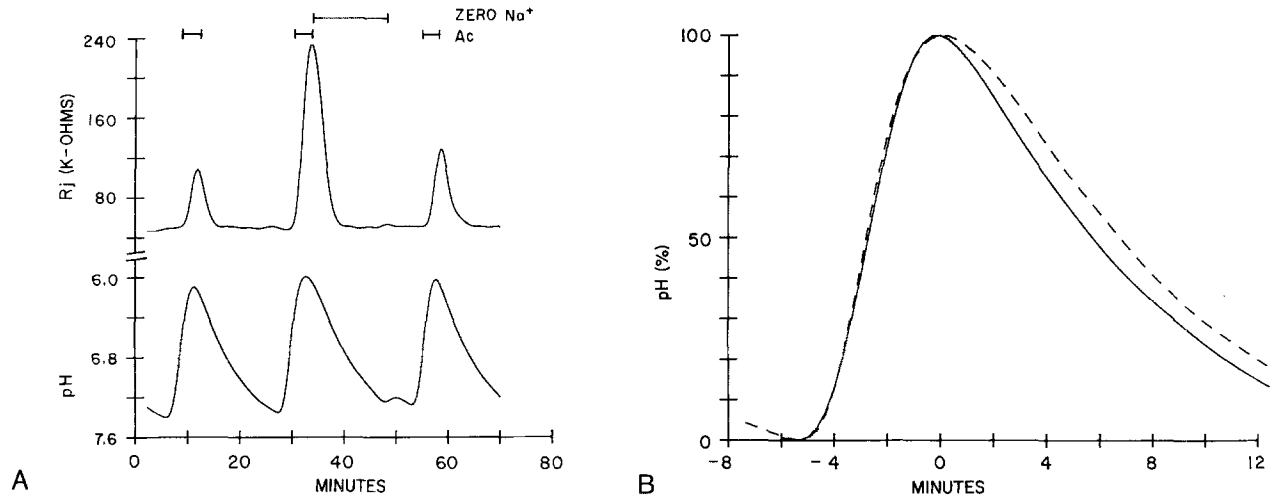

Fig. 8. (*A*) Time course of changes in R_j and pH_i in crayfish axons exposed to zero-Na^+ solutions following Ac treatment. Note that in spite of the fact that the pH minimum reached in the II Ac (recovery in zero-Na) is only slightly more acidic then in the two controls, the R_j maximum of the II Ac is three times greater than controls. In addition, the R_j maximum of the III Ac is slightly greater than that of the I Ac indicating that after exposure to zero-Na^+ the efficiency of Ac-induced uncoupling is increased. (*B*) Superimposition of pH_i curves from I (solid curve) and II (dashed curve) Ac treatment. Note that the zero-Na^+ solution does not inhibit recovery (dashed curve). Recovery of $[H^+]_i$ in both control (I and III Ac) and zero-Na^+ (II Ac) conditions follows a single exponential decay with a similar time constant (τ = 4.4, 4.6, and 4.3 min for I, II and III Ac, respectively)

Ac induced acidification is mostly a passive phenomenon in which H^+ is carried in and out of the cell primarily by the hydrogen-associated form of acetic acid.

In spite of having only minimal effects on the magnitude and duration of pH_i minima, zero-Na^+ recovery solutions cause R_j maxima approximately three times greater than controls (Fig. 8*A*). In addition, Ac treatments performed after zero-Na superfusion cause R_j changes slightly greater than those from similar treatments performed before zero-Na superfusion (compare I and III R_j peaks in Fig. 8*A*). This indicates that the removal of Na_o^+ enhances the uncoupling efficiency of cytoplasmic acidification.

Changes in R_j and Ca_i^{2+} during Acidification

Experiments in which Ca-sensitive microelectrodes rather than pH-microelectrodes were used, show that with Ac there is an increase in $[Ca^{2+}]_i$ of approximately one order of magnitude (Fig. 9*B*; *see also* Figs. 12*B* and *C*, 13*B* and *C*). SES and Ac solutions containing different $[Ca^{2+}]$, ranging from 5 to 40 mM, did not affect the magnitude of the $[Ca^{2+}]_i$ changes (*data not shown*).

R_j and pCa_i curves are similar in shape and their maxima coincide in time (Fig. 9*C*), such that the relationship between pCa and R_j for both decreasing and increasing pCa does not show significant hysteresis (Figs. 9*D* and 11*B*). When the changes in intracellular calcium are expressed as $[Ca^{2+}]_i$ rather than pCa_i, R_j and $[Ca^{2+}]_i$ curves are virtually superimposed (Figs. 9*E* and 12*A*), such that the relationship between $[Ca^{2+}]_i$ and R_j is almost linear in both the uncoupling and recoupling direction (Figs. 9*F*, 11*A*, and 12*B* and *C*). Both R_j and $[Ca^{2+}]_i$ recover following a single exponential decay with a time constant (τ) of ~2.3 min (Fig. 10). These findings have been very consistent in all the experiments that used Ca^{2+}-microelectrodes of short response time (Fig. 11). With slower microelectrodes, R_j and $[Ca^{2+}]_i$ curves were still similar in shape but the $[Ca^{2+}]_i$ maxima lagged slightly behind the R_j maxima.

Fig. 9. Time course of changes in electrotonic potentials, pCa, $[Ca^{2+}]_i$ and R_j in crayfish axons uncoupled with Ac. (*A*) Low speed chart recording of electronic potentials in the posterior (upper trace) and anterior (lower trace) axon segment. (*B*) Low speed chart recording of pCa_i continuously monitored in the anterior axon and plotted as $V_{ion}-V_m$ after filtering (0.1 Hz). (*C*) Time course of percent changes in pCa_i (dashed line) and R_j (solid line) during the I Ac. Note that pCa_i and R_j peaks occur synchronously, and the two curves are similar in shape. (*D*) Relationship between pCa_i and R_j (in percentages) during the I Ac. Note the virtual absence of hysteresis. (*E*) Time course of percent changes in $[Ca^{2+}]_i$ (dashed line) and R_j (solid line) during the I Ac. Note that R_j and $[Ca^{2+}]_i$ curves are virtually superimposed, suggesting a close relationship between Ca^{2+} and R_j. (*F*) Relationship between $[Ca^{2+}]_i$ and R_j (in percentages) during the I Ac. Note the fairly linear relationship between $[Ca^{2+}]_i$ and R_j

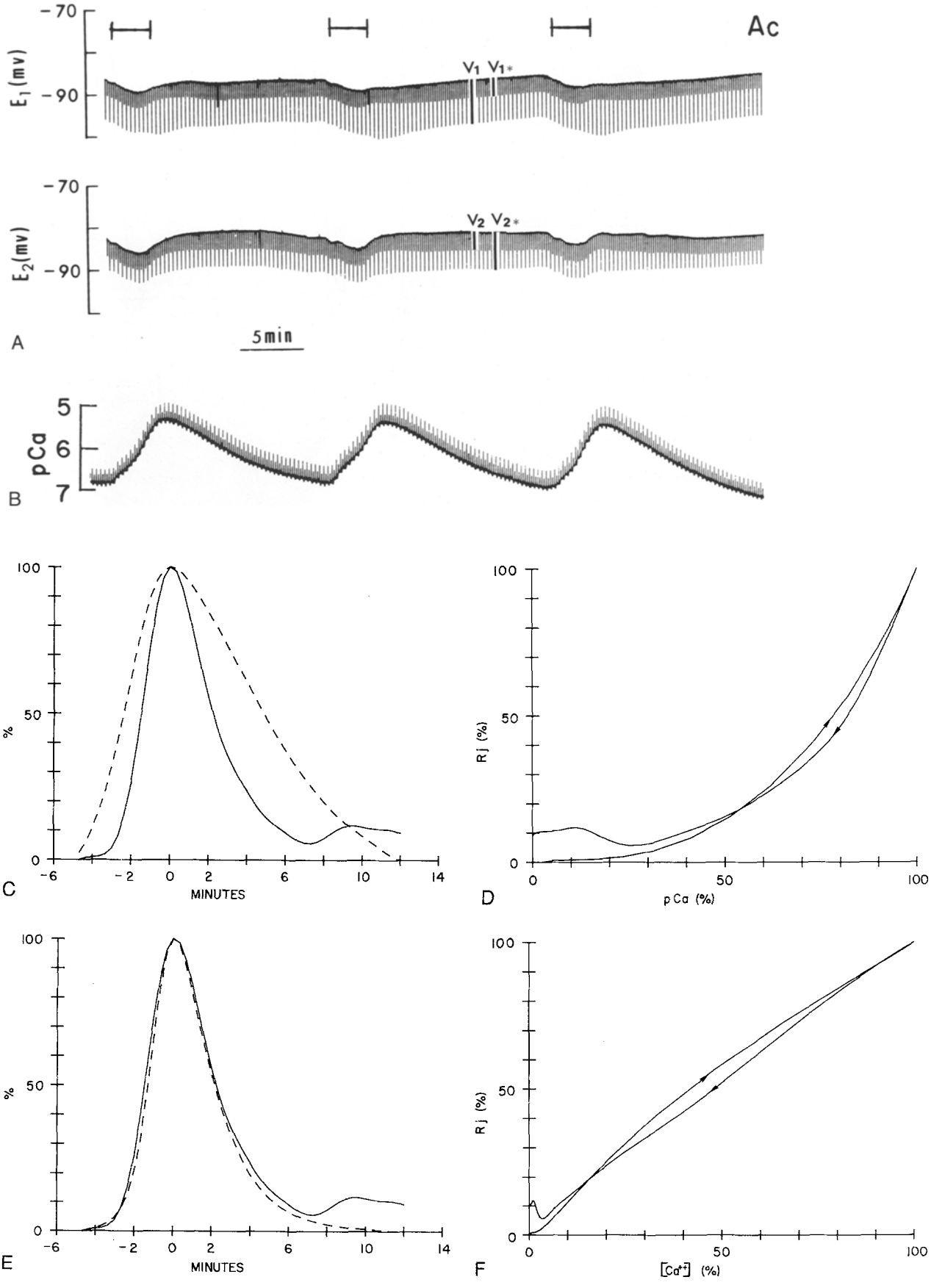
-70
-90
E1(mv)
Ac
V1 V1*
-70
-90
E2(mv)
V2 V2*
A
5min
5
6
7
pCa
B
100
50
0
%
-6 -2 0 2 6 10 14
MINUTES
C
100
50
0
Rj (%)
0 50 100
pCa (%)
D
100
50
0
%
-6 -2 0 2 6 10 14
MINUTES
E
100
50
0
Rj (%)
0 50 100
[Ca++] (%)
F

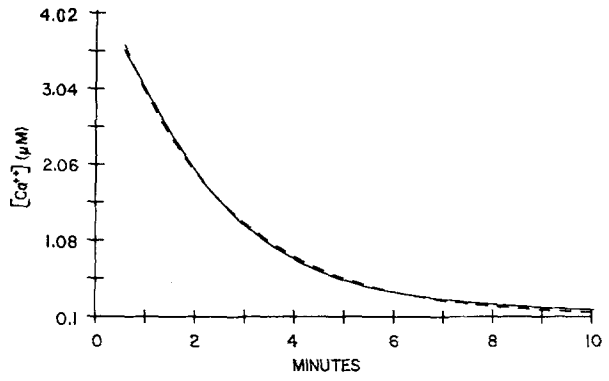

Fig. 10. Time course of $[Ca^{2}]_i$ recovery during the I Ac uncoupling of Fig. 9. The $[Ca^{2+}]_i$ curve is plotted as solid line, the least square exponential fitting as dashed line. Both $[Ca^{2+}]_i$ and R_j (*not shown*) recover to control values following a single exponential decay with a $\tau = \sim 2.3$ min

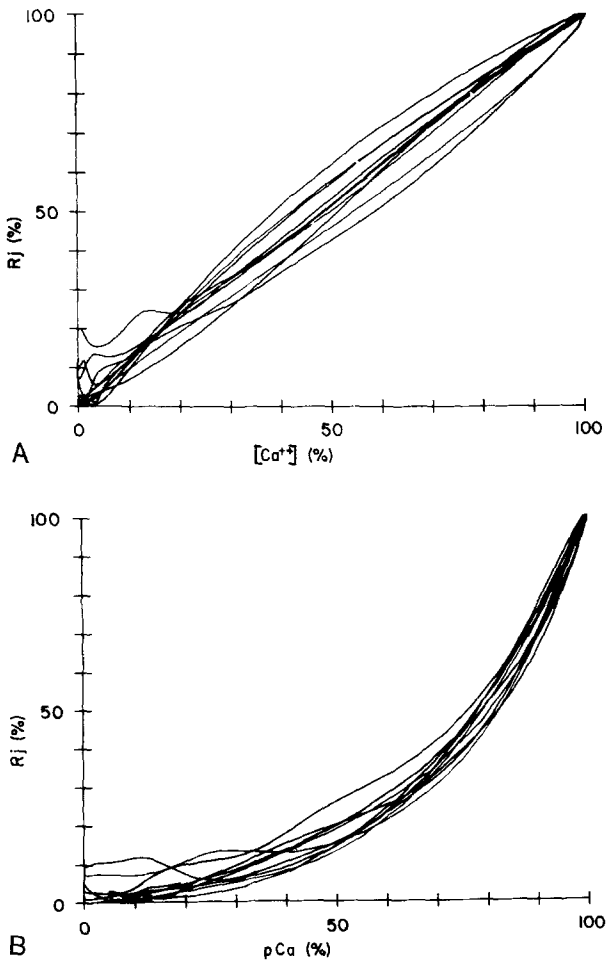

Fig. 11. Computer generated superimposition of several curves, from different experiments, describing the $[Ca^{2+}]_i$–R_j (*A*) or pCa_i–R_j (*B*) relationship (in percentages) during Ac-induced uncoupling events. Note the consistency of the phenomenon in different experiments and the fairly linear relationship between $[Ca^{2+}]_i$ and R_j (*A*)

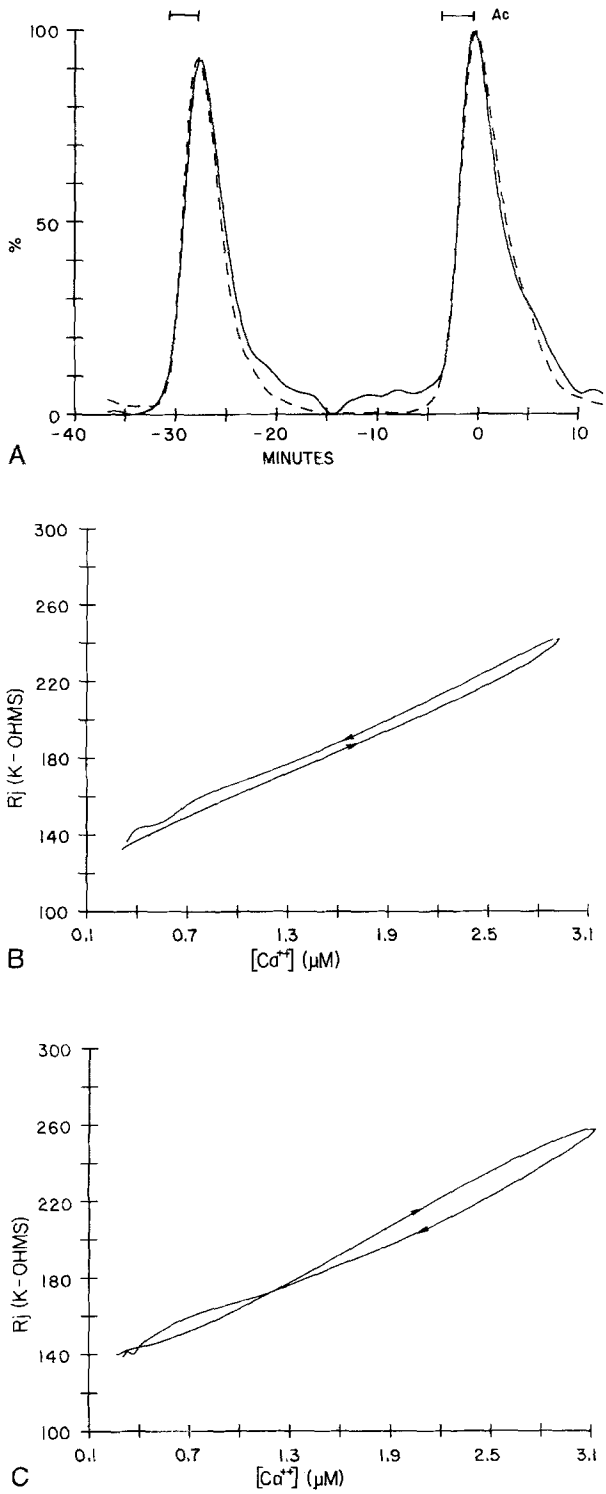

Fig. 12. Time course of percent changes in $[Ca^{2+}]_i$ (dashed line) and R_j (solid line) during two Ac-induced uncoupling events. Note that $[Ca^{2+}]_i$ and R_j curves match well both in shape and in amplitude. Both $[Ca^{2+}]_i$ and R_j maxima of the I Ac are ~7% smaller than those of the II Ac. (*B* and *C*) $[Ca^{2+}]_i$–R_j relationships during I and II Ac, respectively. Note the fairly linear relationship between $[Ca^{2+}]_i$ and R_j. The arrowheads indicate the temporal sequence of uncoupling (up) and recoupling (down)

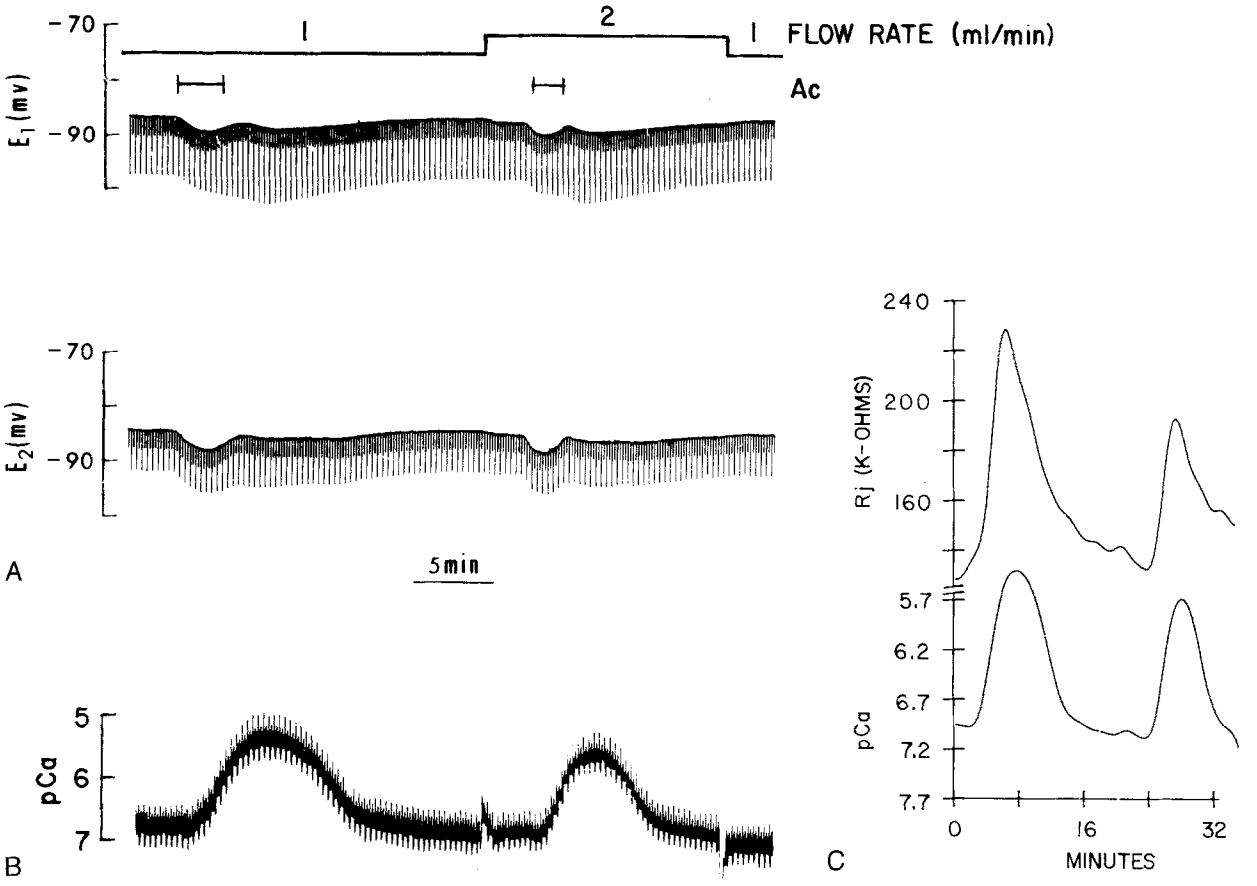

Fig. 13. Time course of changes in electrotonic potentials (*A*), pCa_i (*B* and *C*) and R_j (*C*) in crayfish axons subjected to different rates of acidification. Ac was superfused either for 3 min at a flow rate of 1 ml/min (usual setting) or for 130 sec at 2 ml/min. This protocol was found to cause similar pH_i minima but much greater R_j maxima with slow acidification rate (3 min at 1 ml/min) (*see* Fig. 7). Differently from pH_i, the pCa_i minimum reached with slow acidification (I Ac) is smaller (greater increase in $[Ca^{2+}]_i$) and more sustained than that with fast acidification (II Ac) (*B* and *C*). In addition, there is a close relationship between R_j and pCa_i changes (*C*). With fast acidification both R_j and $[Ca^{2+}]_i$ maxima are 40–50% smaller than with slow acidification

R_j and $[Ca^{2+}]_i$ maxima were also closely related to each other in amplitude. In Fig. 12*A*, for example, the increase in both $[Ca^{2+}]_i$ and R_j during the first Ac exposure is ~7% smaller than that during the second exposure. Similar correspondence between $[Ca^{2+}]_i$ and R_j was seen in experiments using different superfusion rates (Fig. 13*C*).

Effects of Fast and Slow Acidifications on Ca_i^{2+} and R_j

With pH-microelectrodes, the R_j maxima achieved with slow pH_i changes were three times greater than those with fast pH_i changes of the same magnitude (Fig. 7*C*), suggesting that H^+ indirectly affects R_j, possibly via Ca^{2+}. To test this hypothesis, the same experimental protocol was used, but pCa_i rather than pH_i was measured. Figure 13 shows that, indeed, with fast Ac superfusions of 130 sec duration both $[Ca^{2+}]_i$ and R_j maxima are 40–50% smaller than those obtained with slow Ac superfusion of 3 min duration. The parallel behavior of $[Ca^{2+}]_i$ and R_j indicates that R_j is a closer function of $[Ca^{2+}]_i$ than of $[H^+]_i$.

Discussion

This study has monitored simultaneously junctional resistance and either pH_i or pCa_i in crayfish septate axons electrically uncoupled by intracellular acidification. The results show that the curves describing the time course of changes in $[H^+]_i$ and R_j differ significantly from each other, both in terms of curve shape and peak time, and that fast and slow changes in $[H^+]_i$ of similar magnitude have markedly different effects on R_j. In contrast, the curves describing the time course of changes in $[Ca^{2+}]_i$ and R_j match well with each other not only in shape and peak

time, but also in percent increase from base line values.

These observations suggest that in crayfish the low pH_i-induced gating of gap junction channels is more closely related to changes in $[Ca^{2+}]_i$ than in $[H^+]_i$, H^+ probably acting primarily as a trigger to Ca^{2+} release, and confirm the hypothesis that Ca^{2+} is a physiological regulator of cell-to-cell coupling (Loewenstein, 1966; Rose & Loewenstein, 1976). Previous data supporting the role of CaM in low pH_i-induced uncoupling of crayfish axons (Peracchia, 1987*b*) and other cells are consistent with the present results and suggest that uncoupling by low pH_i may result from Ca^{2+} activation of a CaM-like protein (reviewed in Peracchia, 1988).

Both the shape of the $[H^+]_i$ curve and the absence of an effect of zero-Na^+ solutions on pH_i recovery suggest that changes in $[H^+]_i$ may result mainly from passive transport of H^+ by undissociated acetic acid, the difference in time course between rising and decaying phase of $[H^+]_i$ possibly being the result of a much smaller gradient of acetate across the membrane in the latter. Although the recovery of $[H^+]_i$ to control values is likely to reflect many factors, including: diffusion of acetic acid in the cytoplasm and through the plasma membrane, binding/unbinding of H^+ to intracellular sites and acetate, diffusion of acetate through the extracellular space, etc., the fact that $[H^+]_i$ recovers following a single exponential function, both in the presence and absence of Na_o^+, indicates that the changes in $[H^+]_i$ reflect mainly one variable, most likely the diffusion of acetic acid across the plasma membrane. This is probably the reason why the $[H^+]_i$ changes with acetate were very consistent in all the experiments in which the same superfusion protocol was employed. On the other hand, other mechanisms could be involved in pH_i recovery from acetate, and this issue has not been explored in sufficient detail in this study to entirely rule out any other mechanism not involving passive diffusion of acetic acid.

The $[H^+]_i$ maxima were seen to precede the R_j maxima by 40–90 sec, but this value represents a conservative estimate. In fact, the $[H^+]_i$ maxima are likely to precede the R_j maxima by an even greater length of time, because the pH electrodes are much slower than the voltage recording electrodes used for measuring R_j.

The observation of large differences in R_j maxima between fast and slow acidifications of similar magnitude also suggests an indirect H^+ effect on gating. Based on data with Ca-microelectrodes, a reasonable interpretation of this finding is that H_i^+ causes an increase in $[Ca^{2+}]_i$ by a mechanism that depends both on $[H^+]_i$ and on the duration of low pH_i. Thus, slow acidifications would cause larger increases in $[Ca^{2+}]_i$ and consequently greater R_j maxima than fast acidifications of similar overall magnitude. This could also explain the large increase in R_j observed with zero-Na^+ recovery solutions. In these cases $[H^+]_i$ maxima were not much greater than in controls, but the low pH_i was more sustained. On the other hand, this phenomenon could also have resulted from the Ca^{2+}-loading effect of zero-Na^+ solutions, via inhibition of Na^+/Ca^{2+} exchange at the plasma membrane.

The relationship between $[Ca^{2+}]_i$ and R_j appears to be almost linear, while one may expect it to follow a curve, eventually reaching a plateau at the highest $[Ca^{2+}]_i$ values. A possible reason for the absence of a plateau is that the $[Ca^{2+}]_i$ maxima obtained with acidification may not be sufficiently high to close all the gap junction channels. If this were the case one would expect to see only an intermediate segment of the $[Ca^{2+}]_i$–R_j relationship as the curve would reach a plateau only at higher $[Ca^{2+}]_i$, when most of the Ca^{2+} sites at the channels are occupied. In fact, in most experiments the R_j maxima were significantly smaller than those theoretically calculated, assuming complete occlusion of all junctional channels. A linear relationship may in fact indicate a one-to-one-relationship between Ca^{2+} and channel gates.

R_j and $[Ca^{2+}]_i$ curves were seen to peak almost synchronously when the Ca-microelectrodes had a fast response. However, in real time it is likely that the $[Ca^{2+}]_i$ changes precede slightly the changes in R_j because even the fastest ion selective microelectrodes are slower than the voltage electrodes from which R_j is calculated. Aside from microelectrode response time, elements such as distance between microelectrode tip and junctions, location of Ca^{2+}-release mechanism and speed of Ca^{2+} diffusion through the axoplasm play a role. In addition, since channel gates are believed to be at both channel ends, the channels are likely to close independently at each end. If $[Ca^{2+}]_i$ does not change synchronously in both axons, R_j is likely to reflect mostly the gating status of the hemichannels of the axon where $[Ca^{2+}]_i$ is greater. However, in experiments in which the Ca^{2+} microelectrode was withdrawn from one of the two axons and inserted into the other, the temporal relationship between $[Ca^{2+}]_i$ and R_j maxima did not change significantly, indicating that indeed the changes in $[Ca^{2+}]_i$ occur fairly synchronously in both axons, at this time scale at least. Another element supporting the close relationship between $[Ca^{2+}]_i$ and junctional conductance is the observed similarity in percent increase in $[Ca^{2+}]_i$ and R_j from base line values.

Whether in other cell systems the H^+ effects on coupling are also mediated by Ca^{2+} is not known. Crayfish septate axons, being cells highly special-

ized for fast conduction, could have an unusual gap junction regulation. Moreover, arthropod gap junctions are structurally different from other gap junctions (Peracchia, 1980). On the other hand, unequivocal evidence for a direct effect of H^+ in any cell system is still lacking.

Early findings seemed to support a direct effect of H^+ on gap junction channels (Spray & Bennett, 1985), but some inconsistencies soon became apparent (Peracchia 1987*a*). In embryonal cells of amphibia, Turin and Warner (1980) showed changes in both coupling ratio V_2/V_1 (α) and pH_i but plotted α versus pH_i only for the recoupling phase, thus a possible curve hysteresis was not determined. Spray et al. (1981) indeed reported a hysteresis in the relationship between pH_i and α in these cells but interpreted it as an artifact of the effects of CO_2 on nonjunctional membrane conductance. The same study reported the absence of hysteresis in the relationship between pH_i and junctional conductance (gj) and thus concluded that protons act directly on the channel macromolecules.

Giaume, Spira and Korn (1980) were the first to demonstrate the uncoupling effects of internal acidification in the crayfish. In a subsequent study (Giaume & Korn, 1982) both pH_i and R_j were measured, but the relationship between the two variables was not investigated. Campos de Carvalho, Spray and Bennett (1984), reported that gj, measured when pH_i decreases, indeed falls nearly along the same Hill relationship as gj measured when pH_i is recovering, but only with brief exposures to acetate (4 min). In contrast, with longer acetate exposures (11 min) gj recovered slowly and incompletely in spite of the fact that pH_i recovered at a normal rate (Campos de Carvalho et al., 1984). Nevertheless, they concluded that also in the crayfish there is a direct relationship between pH_i and gj (Campos de Carvalho et al., 1984). However, the recessed-tip pH microelectrodes used in this study were not very fast, the reported response time for 1 pH unit change being typically 1 min (Campos de Carvalho et al., 1984). These authors assumed that pH_i and gj minima coincided in real time and accordingly normalized in time gj and pH_i minima before plotting the relationship between pH_i and gj. The two curves apparently matched, at least for brief acetate exposures, but any possible hysteresis due to the absence of synchronism between pH_i and gj minima was eliminated. In any event, our data show that substantial hysteresis would be present also if, for the sake of argument, $[H^+]_i$ and R_j maxima were normalized, because the recovery rate of $[H^+]_i$ has a time constant approximately twice as long as that of R_j. In addition, we did not see any significant difference in R_j recovery rate between shorter (130 sec to 3 min) and longer (5–10 min) exposures to acetate, substantial hysteresis being present in both cases.

The pH_i sensitivity of coupling has been found to vary in different systems and even in the same cells. Turin and Warner (1980) showed that in amphibian embryonal cells a 50% recovery of α from CO_2 treatments occurs at pH_i 6.5 in some experiments and at $pH_i = 6.9$ in other. In other cells the pK of the Hill plot ranged widely from 7.3 to 6.3 (Spray & Bennett, 1985). In addition, the Hill curve varied considerably in steepness, ranging from a maximum in hepatocytes ($N > 5$) to a minimum in cardiac myocytes ($N = \sim 1$) (Spray & Bennett, 1985), a pH_i of 6.6 had only a small effect in mammalian heart fibers (Reber & Weingart, 1982), H^+ affected healing-over in the heart only at a pH lower than 5 (DeMello, 1983), and low-pH solutions did not change junctional conductance in internally perfused crayfish axons (Johnston & Ramón, 1981; Arellano et al., 1986). Moreover, low pH did not alter the permeability of lens gap junction channels incorporated into planar bilayers (Zampighi, Hall & Kreman, 1985) and failed to produce the closed channel configuration in isolated junctions (Unwin & Ennis, 1983). Several inconsistencies between pH_i and electrical coupling were also reported in cells of insect salivary glands (Rose & Rick, 1978) and this study showed that Ca^{2+} is sufficient to close the channels in physiological conditions. On the other hand, the possibility that H^+ directly affects gating in some systems cannot be entirely ruled out. This may be the case in fish blastomeres, where R_j increased with internally perfused low-pH solutions at low $[Ca^{2+}]$ (Spray et al., 1982).

The increase in $[Ca^{2+}]_i$ in response to acidification may be the result of Ca^{2+} release from Ca^{2+}-binding sites and/or intracellular stores. This seems likely because different $[Ca^{2+}]_o$ did not change $[Ca^{2+}]_i$ and R_j maxima with Ac, suggesting the absence of a significant increase in Ca^{2+} influx. Intracellular sources of Ca^{2+}, are the endoplasmic reticulum, mitochondria, Ca^{2+}-binding sites and calciosomes. Calciosomes are believed to be 0.1 μm vesicles, located near the plasma membrane of various cells, that contain calsequestrin like terminal cisternae of sarcoplasmic reticulum (SR) (Volpe et al., 1988). Interestingly, the gap junctions of crayfish septate axons are covered on both surfaces with 50–80 nm vesicles (Peracchia, 1973), believed to be Ca^{2+}-sequestering organelles anchored to the junctions to maintain the channels in a low $[Ca^{2+}]$ environment (Peracchia & Dulhunty, 1976); however, other hypotheses for the function of the vesicles have also been formulated (Peracchia, 1973; Zampighi et al., 1988).

While there is a no evidence yet that calciosomes release Ca^{2+} with acidification, a H^+-induced

Ca^{2+} release from the SR of barnacle muscles has been reported (Lea & Ashley, 1981). In this study, Ca^{2+} release occurred only when acidification followed exposure to CO_2 or weak acids and did not depend on acidification of the cytoplasmic free-medium but rather on acidification of the luminal medium of SR cisternae. Based on these data, one may think that the increase in $[Ca^{2+}]_i$ with Ac could be caused by a diffusion of the H^+-associated form of acetate into Ca^{2+}-storing compartments. If this were the case, one would expect that cytoplasmic acidification caused by weak acids, CO_2, ammonium chloride washout, etc., would induce greater $[Ca^{2+}]_i$ release and larger increase in R_j than that caused by intracellular injection of poorly permeant acids (strong acids). Indeed, junctional conductance was found to decrease at pH_i lower than 6.8 in cells exposed to CO_2, but only at pH_i lower than 5.8 in cells injected with HCl (Bennett et al., 1988). Consistent with the hypothesis of H^+-induced Ca^{2+} release from reticulum are preliminary data on the effects of caffeine and ryanodine on changes in R_j and $[Ca^{2+}]_i$ with Ac in crayfish (Peracchia, 1989*b*). Aside from intracellular compartments, plasma membrane ion exchange mechanisms may also contribute, as an increase in $[H^+]_i$ would stimulate Na^+/H^+ exchange and the resulting increase in $[Na^+]_i$ would inhibit Ca^{2+} extrusion via Na^+/Ca^{2+} exchange. These mechanisms may play a role in maintaining cell uncoupling and high $[Ca^{2+}]_i$ during prolonged acidification.

Cytoplasmic acidification has been shown to affect $[Ca^{2+}]_i$ in various other cells. $[Ca^{2+}]_i$ was found to increase with lowered pH_i in squid giant axons (Mullins et al., 1983; Requena et al., 1986), in molluscan neurons (Ahmed & Connor, 1980), in barnacle muscle (Lea & Ashley, 1981), in salivary gland cells of insects (Rose & Rick, 1978) and in *Xenopus* embryonal cells (Rink, Tsien & Warner, 1980). In mammalian heart, $[Ca^{2+}]_i$ was first reported to decrease with acidification (Hess & Weingart, 1980; Reber & Weingart, 1982), but more recent studies reported it to increase (Bers & Ellis, 1982; Allen, Eisner & Orchard, 1984; Kaila, Vaughan-Jones & Bountra, 1987; Vaughan-Jones, Eisner & Lederer, 1987). In most systems $[Ca^{2+}]_i$ increased less than in crayfish axons with acidification; however, in most cases the values of pH_i tested were not as low as those achieved with Ac.

In this study, Ca^{2+} appears to affect the channel gates at nanomolar concentrations. In the past, the $[Ca^{2+}]_i$ effective on coupling has been a matter of controversy. While $[Ca^{2+}]_i$ as high as 40–400 μM were reported to have an effect in most ruptured (Oliveira-Castro & Loewenstein, 1971) or internally perfused (Spray et al., 1982) cells, low micromolar concentrations were reported effective in various intact cells (Rose & Loewenstein, 1976; Weingart, 1977; Dahl & Isenberg, 1980; Neyton & Trautmann, 1986; Maurer & Weingart, 1987). It has been previously suggested (Johnston & Ramón, 1981) that the low calcium sensitivity of ruptured or perfused cells might have resulted from the loss of a cytoplasmic intermediate; the intermediate could be a CaM-like protein (Peracchia, 1988).

In conclusion, this study shows lack of a direct relationship between intracellular pH and channel gating in crayfish septate axons. In these cells intracellular acidification causes an increase in $[Ca^{2+}]_i$ that closely matches a parallel increase in junctional resistance. This suggests that acidification may close these gap junction channels via changes in internal free calcium. Whether the same mechanism takes place in other cell systems remains to be proven.

The author wishes to thank Drs. Peter G. Shrager, Trevor J. Shuttleworth and Thomas E. Gunter for helpful criticism, Drs. Shey-Shing Sheu and Daniel J. Williford for providing Ca-cocktails and for sharing their knowledge on ion selective microelectrodes, Mr. John Trueswell and Dr. Patricia Donaldson for writing the computer program, and Ms. Lillian M. Peracchia for excellent technical help. This study was supported by NIH grant GM 20113.

References

Ahmed, Z., Connor, J.A. 1980. Intracellular pH changes induced by calcium influx during electrical activity in molluscan neurons. *J. Gen. Physiol.* **75**:403–426

Allen, D.G., Eisner, D.A., Orchard, C.H. 1984. Characteristics of oscillation of intracellular calcium concentration in ferret ventricular muscle. *J. Physiol. (London)* **352**:113–128

Alvarez-Leefmans, F.J., Rink, T.J., Tsien, R.Y. 1981. Free calcium ions in neurons of *Helix aspersa* measured with ion-selective microelectrodes. *J. Physiol. (London)* **315**:531–438

Ammann, D., Lanter, F., Steiner, R.A., Schulthess, P., Shijo, Y., Simon, W. 1981. Neutral carrier based hydrogen ion selective microelectrode for extra- and intracellular studies. *Anal. Chem.* **53**:2267–2269

Ammann, D., Oesch, U., Bührer, T., Simon, W. 1987. Design of ionophores for ion-selective microsensors. *Can. J. Physiol. Pharmacol.* **65**:879–884

Arellano, R.O., Ramón, F., Rivera, A., Zampighi, G.A., 1986. Lowering of pH does not directly affect the junctional resistance of crayfish lateral axons. *J. Membrane Biol.* **94**:293–299

Arellano, R.O., Ramón, F., Rivera, A., Zampighi, G.A. 1988. Calmodulin acts as an intermediary for the effects of calcium on gap junctions from crayfish lateral axons. *J. Membrane Biol.* **101**:119–131

Bennett, M.V.L. 1966. Physiology of electronic junctions. *Ann. N.Y. Acad. Sci.* **37**:509–539

Bennett, M.V.L., Verselis, R.L., White, R.L., Spray, D.C. 1988. Gap junctional conductance: Gating . *In:* Gap Junctions. E.L. Hertzberg and R.G. Johnson editors. pp. 207–304. Alan R. Liss, New York

Bers, D.M., Ellis, D. 1982. Intracellular calcium and sodium activity in sheep cardiac Purkinje fibers: Effects of changes of external sodium and intracellular pH. *Pfluegers Arch.* **393:**171–178

Campos de Carvalho, A., Spray, D.C., Bennett, M.V.L. 1984. pH dependence of transmission at electronic synapses of the crayfish septate axon. *Brain Res.* **321:**279–286

Dahl, G., Isenberg, G. 1980. Decoupling of heart muscle cells: Correlation with increased cytoplasmic calcium activity and with changes of nexus ultrastructure. *J. Membrane Biol.* **53:**63–75

DeMello, W.C. 1983. The influence of pH on the healing-over of mammalian cardiac muscle. *J. Physiol. (London)* **339:**299–307

Giaume, C., Korn, H. 1982. Ammonium sulfate induced uncouplings of crayfish septate axons with and without increased junctional resistance. *Neuroscience* **7:**1723–1730

Giaume, C., Spira, M.E., Korn, H. 1980. Uncoupling of invertebrate electronic synapses by carbon dioxide. *Neurosci. Lett.* **17:**197–202

Girsch, S.J., Peracchia, C. 1985. Lens cell-to-cell channel protein: I. Self-assembly into liposomes and permeability regulation by calmodulin. *J. Membrane Biol.* **83:**217–225

Hess, P., Weingart, R. 1980. Intracellular free calcium modified by pH_i in sheep cardiac Purkinje fibres. *J. Physiol. (London)* **307:**60P–61P

Johnston, M.F., Ramón, F. 1981. Electronic coupling in internally perfused crayfish segmented axons. *J. Physiol. (London)* **317:**509–518

Kaila, K., Vaughan-Jones, R.D., Bountra, C. 1987. Rgulation of intracellular pH in sheep cardiac Purkinje fibre: Interactions among Na^+, H^+ and Ca^{++}. *Can. J. Physiol. Pharmacol.* **65:**963–969

Lasater, E.M., Dowling, J.E. 1985. Dopamine decreases conductance of the electrical junctions between cultured retinal horizontal cells. *Proc. Natl. Acad. Sci. USA* **82:**3025–3029

Lea, T.J., Ashley, C.C. 1981. Carbon dioxide or bicarbonate ions release Ca^{2+} from internal stores in Crustacean myofibrillar bundles. *J. Membrane Biol.* **61:**115–125

Loewenstein, W.R. 1966. Permeability of membrane junctions. *Ann. N.Y. Acad. Sci.* **137:**441–472

Loewenstein, W.R. 1981. Junctional intercellular communication: The cell-to-cell membrane channel. *Physiol. Rev.* **61:**829–913

Maurer, P., Weingart, R. 1987. Cell pairs isolated form adult guinea pig and rat hearts: Effects of $[Ca^{++}]_i$ on nexal membrane resistance. *Pfluegers Arch.* **409:**394–402

Mullins, L.J., Tiffert, T., Vassort, G., Whittembury, J. 1983. Effects of internal sodium and hydrogen-ions and of external calcium-ions and membrane potential on calcium entry in squid axons. *J. Physiol. (London)* **338:**295–319

Neyton, J., Trautmann, A. 1986. Acetylcholine modulation of the conductance of intercellular junctions between rat lacrimal cells. *J. Physiol. (London)* **337:**283–295

Oliveira-Castro, G.M., Loewenstein, W.R. 1971. Junctional membrane permeability: Effects of divalent cations. *J. Membrane Biol.* **5:**51–77

Peracchia, C. 1973. Low resistance junctions in crayfish: I. Two arrays of globules in junctional membranes. *J. Cell Biol.* **57:**54–65

Peracchia, C. 1980. Structural correlates of gap junction permeation. *Int. Rev. Cytol.* **66:**81–146

Peracchia, C. 1984. Communicating junctions and calmodulin: Inhibition of electrical uncoupling in *Xenopus* embryo by calmidazolium. *J. Membrane Biol.* **81:**49–58

Peracchia, C. 1987*a*. Permeability and regulation of gap junction channels in cells and in artificial lipid bilayers. *In:* Cell-to-Cell Communication. W.C. DeMello, editor. pp. 65–102. Plenum, New York

Peracchia, C. 1987*b*. Calmodulin-like proteins and communicating junctions—electrical uncoupling of crayfish septate axons is inhibited by the calmodulin inhibitor W7 and is not affected by cyclic nucleotides. *Pfluegers Arch.* **408:**379–385

Peracchia, C. 1988. The calmodulin hypothesis for gap junction regulation six years later. *In:* Gap Junctions. E.L. Hertzberg, and R.G. Johnson, editors. pp. 267–282. Alan R. Liss, New York

Peracchia, C. 1989*a*. Changes in Ca^{++}, H^+ and junctional resistance in crayfish axons uncoupled by acidification. *Biophys. J.* **55:**151a

Peracchia, C. 1989*b*. Participation of caffeine- and ryanodine-sensitive Ca^{++}-stores in low pH_i-induced uncoupling of crayfish axons. *Soc. Neurosci. Abstr.* **15(Part 2):**1302

Peracchia, C., Bernardini, G., Peracchia, L.L. 1983. Is calmodulin involved in the regulation of gap junction permeability? *Pfluegers Arch.* **399:**152–154

Peracchia, C., Dulhunty, A.F. 1976. Low resistance junctions in crayfish. Structural changes in functional uncoupling. *J. Cell Biol.* **70:**419–439

Ramón, F., Rivera, A. 1987. Gap junction channel modulation. A physiological viewpoint. *Prog. Biophys.* **48:**127–153

Reber, W.R., Weingart, R. 1982. Ungulate cardiac Purkinje fibres: The influence of intracellular pH on the electrical cell-to-cell coupling. *J. Physiol. (London)* **328:**87–104

Requena, J., Mullins, L.J., Whittembury, J., Brinley, F.J., Jr. 1986. Dependence of ionized and total Ca in squid axons on Na_o-free or high-K_o conditions. *J. Gen. Physiol.* **87:**143–159

Rink, T.J., Tsien, R.-Y., Warner, A.E. 1980. Free calcium in *Xenopus* embryos measured with ion-selective microelectrodes. *Nature (London)* **283:**658–660

Rose, B., Loewenstein, W.R. 1976. Permeability of a cell junction and the local cytoplasmic free ionized calcium concentration: A study with aequorin. *J. Membrane Biol.* **28:**87–119

Rose, B., Rick, R. 1978. Intracellular pH, intracellular free Ca, and junctional cell-cell coupling. *J. Membrane Biol.* **44:**377–415

Schefer, U., Ammann, D., Pretsch, E., Oesch, U., Simon, W. 1986. Neutral carrier based Ca^+-selective electrode with detection limit in the subnanomolar range. *Anal. Chem.* **58:**2282–2285

Schulthess P., Shijo, Y., Pham, H.V., Pretsch, E., Ammann, D., Simon, W. 1981. A hydrogen ion-selective liquid membrane electrode based on tri-*n*-dodecylamine as neutral carrier. *Anal. Chim. Acta* **131:**111–116

Spray, D.C., Bennett, M.V.L. 1985. Physiology and pharmacology of gap junctions. *Annu. Rev. Physiol.* **47:**281–303

Spray, D.C., Harris, A.L., Bennett, M.V.L. 1981. Gap junctional conductance is a simple and sensitive function of intracellular pH. *Science* **211:**712–715

Spray, D.C., Stern, J.H., Harris, A.L., Bennett, M.V.L. 1982. Gap junctional conductance: Comparison of sensitivities to H and Ca ions. *Proc. Natl. Acad. Sci. USA* **79:**441–445

Turin, L., Warner, A.E. 1977. Carbon dioxide reversibly abolishes ionic communication between cells of early embryo. *Nature (London)* **270:**56–57

Turin, L., Warner, A.E. 1980. Intracellular pH in early *Xenopus* embryos: Its effect on current flow between blastomeres. *J. Physiol. (London)* **300:**489–504

Unwin, P.N.T., Ennis, P.D. 1983. Calcium-mediated changes in gap junction structure: Evidence from the low angle X-ray pattern. *J. Cell. Biol.***97:**1459–1466

Vaughan-Jones, R.D., Eisner, D.A., Lederer, W.J. 1987. Effects of changes of intracellular pH on contraction in sheep cardiac Purkinje fibers. *J. Gen. Physiol.* **89:**1015–1032

Volpe, P., Krause, K.-H., Hashimoto, S., Zorzato, F., Pozzan, T., Meldolesi, J., Lew, D.P. 1988. "Calciosome," a cytoplasmic organelle: The inositol 1, 4, 5-triphosphate-sensitive Ca^{++} store of non muscle cells? *Proc. Natl. Acad. Sci. USA* **85:**1091–1095

Weingart, R. 1977. Action of ouabain on intercellular coupling and conduction-velocity in mammalian ventricular muscle. *J. Physiol. (London)* **264:**341–365

Zampighi, G.A., Hall, J.E., Kreman, M. 1985. Purified lens junctional protein forms channels in planar lipid films. *Proc. Natl. Acad. Sci. USA* **82:**8468–8472

Zampighi, G.A., Kreman, M., Ramón, F., Moreno, A.L., Simon, S.A. 1988. Structural characteristics of gap junctions: I. Channel number in coupled and uncoupled conditions. *J. Cell Biol.* **106:**1667–1678

Received 29 June 1989; revised 1 September 1989